AGU PUBLICATIONS

JGR

Journal of Geophysical Research: Biogeosciences

RESEARCH ARTICLE
10.1002/2014JG002832

Key Points:
- Dissolved organic carbon (DOC) dynamics were measured in an alluvial aquifer
- Total and humic DOC decline while labile DOC increases with residence time
- Particulate organic matter and methane are potential sources of labile DOC

Supporting Information:
- Supporting Information S1

Correspondence to:
A. M. Helton,
ashley.helton@uconn.edu

Citation:
Helton, A. M., M. S. Wright, E. S. Bernhardt, G. C. Poole, R. M. Cory, and J. A. Stanford (2015), Dissolved organic carbon lability increases with water residence time in the alluvial aquifer of a river floodplain ecosystem, *J. Geophys. Res. Biogeosci.*, *120*, 693–706, doi:10.1002/2014JG002832.

Received 19 OCT 2014
Accepted 9 MAR 2015
Accepted article online 17 MAR 2015
Published online 23 APR 2015

Dissolved organic carbon lability increases with water residence time in the alluvial aquifer of a river floodplain ecosystem

Ashley M. Helton[1], Meredith S. Wright[2], Emily S. Bernhardt[3], Geoffrey C. Poole[4,5], Rose M. Cory[6], and Jack A. Stanford[7]

[1]Department of Natural Resources and the Environment and the Center for Environmental Sciences and Engineering, University of Connecticut, Storrs, Connecticut, USA, [2]J. Craig Venter Institute, La Jolla, California, USA, [3]Biology Department, Duke University, Durham, North Carolina, USA, [4]Department of Land Resources and Environmental Sciences, Montana State University, Bozeman, Montana, USA, [5]Montana Institute on Ecosystems, Montana State University, Bozeman, Montana, USA, [6]Earth and Environmental Sciences, University of Michigan, Ann Arbor, Michigan, USA, [7]Flathead Lake Biological Station, Division of Biological Sciences, University of Montana, Missoula, Montana, USA

Abstract We assessed spatial and temporal patterns of dissolved organic carbon (DOC) lability and composition throughout the alluvial aquifer of the 16 km^2 Nyack Floodplain in northwest Montana, USA. Water influx to the aquifer derives almost exclusively from the Middle Fork of the Flathead River, and water residence times within the aquifer range from days to months. Across seasons and channel discharge conditions, we measured DOC concentration, lability, and optical properties of aquifer water sampled from 12 wells, both near and ~3 m below the water table. Concentrations of DOC were typically low (542 ± 22.7 $\mu g\ L^{-1}$; mean ± se), and the percentage of labile DOC averaged 18 ± 12% during 3 day laboratory assays. Parallel factor analysis of fluorescence excitation-emission matrices revealed two humic-like and two amino acid-like fluorescence groups. Total DOC, humic-like components, and specific UV absorbance decreased with water residence time, consistent with sorption to aquifer sediments. However, labile DOC (both concentration and fraction) increased with water residence time, suggesting a concurrent influx or production of labile DOC. Thus, although the carbon-poor, oxygen-rich aquifer is a net sink for DOC, recalcitrant DOC appears to be replaced with more labile DOC along aquifer flow paths. Our observation of DOC production in long flow paths contrasts with studies of hyporheic DOC consumption along short (centimeters to meters) flow paths and highlights the importance of understanding the role of labile organic matter production and/or influx in alluvial aquifer carbon cycling.

1. Introduction

Because subterranean aquifer ecosystems lack phototrophic primary production, organic matter influx from floodplains and rivers is typically assumed to be the primary energy source for alluvial aquifer ecosystems [*Gibert and Deharveng*, 2002; *Datry et al.*, 2005]. The soil, vadose zone, and streambed sediments act as strong filters for particulate organic matter (POM), leaving dissolved organic carbon (DOC) as the major form of carbon supplied to aquifer interiors [*Starr and Gillham*, 1993; *Boulton*, 2000]. Researchers have consistently observed declines in DOC concentrations and lability along short, well-constrained hyporheic flow paths (centimeters to meters), indicative of efficient microbial uptake of labile DOC during infiltration of river channel water [e.g., *Hedin et al.*, 1998; *Sobczak and Findlay*, 2002; *Zarnetske et al.*, 2011].

Extrapolating these findings to longer alluvial aquifer flow paths of large river floodplains suggests that labile DOC should be consumed quickly along flow paths, leaving less and poorer quality DOC to support ecosystems as hydraulic residence time increases along aquifer flow paths. Such a conceptual model is inconsistent with observations that deeper hyporheic and aquifer flow paths can support diverse and abundant invertebrate communities [*Williams and Hynes*, 1974; *Danielopol*, 1989; *Stanford et al.*, 1994], with potentially high rates of secondary production [*Reynolds and Benke*, 2012]. Alternative sources of carbon to aquifer interiors, such as buried POM breakdown [*Gurwick et al.*, 2008] or methanotrophic production [*Shelley et al.*, 2014], may explain the energy balance of these aquifer food webs.

Here we examined spatial and temporal patterns of DOC concentration, lability, and composition in the alluvial aquifer of Nyack Floodplain on the Middle Fork of the Flathead River, Montana, USA, which has been a

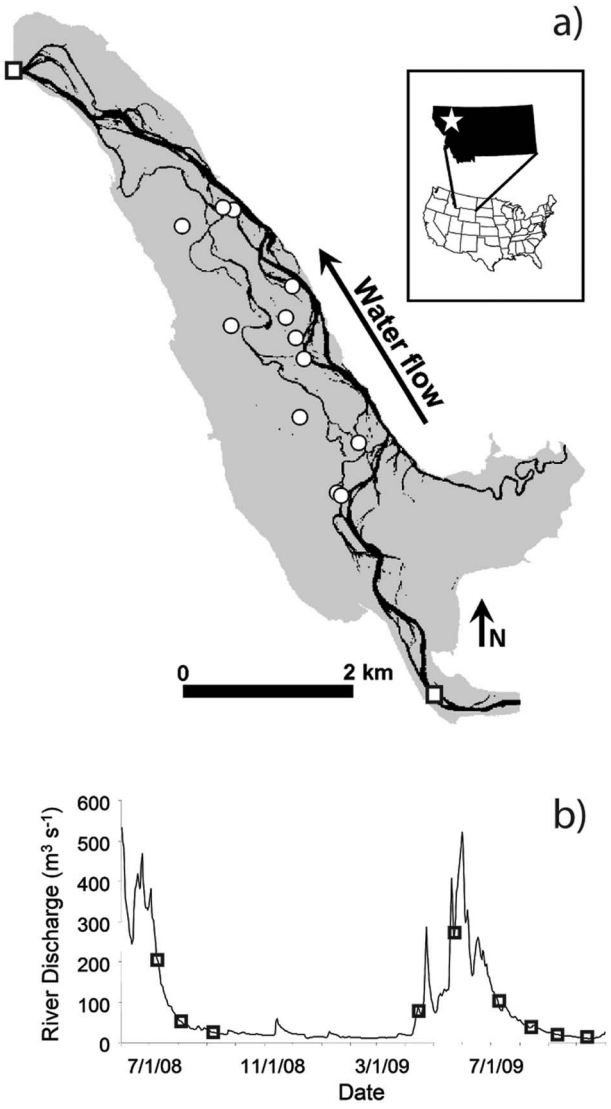

Figure 1. (a) Plan view of Nyack Floodplain extent on the Middle Fork Flathead River located in northwest Montana, USA (shown in inset). White circles indicate well locations, and white squares indicate river water sampling locations. Black area is surface water extent. (b) Hydrograph of the Middle Fork Flathead River at U.S. Geological Survey Gage #12358500. Open squares indicate sampling dates.

research site for hyporheic ecology for more than three decades. Despite severe carbon limitation to microbial communities [*Ellis et al.*, 1998; *Craft et al.*, 2002], an extensive food web with over 70 taxa of interstitial invertebrates exists within the alluvial aquifer [*Stanford et al.*, 1994]. Prior estimates of high macroinvertebrate abundance and biomass [*Reid*, 2007] exceed that which would be expected from low measured inputs of riverine DOC. Thus, the commonly held conceptual model of depletion of recently derived labile DOC as the primary energy source along flow paths may not apply to the longer (multiple kilometers) flow paths of this alluvial aquifer.

To examine whether the conceptual model of depletion of labile DOC with hydraulic residence time applies to the Nyack aquifer, we combined measurements of DOC concentration, lability from laboratory incubations, and optical properties, including parallel factor analysis (PARAFAC) of fluorescence excitation-emission matrices, with a newly developed model of hydraulic residence time for the Nyack aquifer [*Helton et al.*, 2014]. Other studies testing this conceptual model have used conservative tracer techniques in combination with DOC concentration and composition measurements [e.g., *Miller et al.*, 2006; *Zarnetske et al.*, 2011]. However, standard tracer techniques quantify only short hydrologic flow paths (hours to days and centimeters to meters) and are inadequate to measure hydrologic transport distances and residence times (tens of meters to kilometers and days to months) in larger alluvial aquifer systems [*Poole et al.*, 2008; *Bencala et al.*, 2011], such as the Nyack. Thus, we used the modeled hydraulic residence times, combined with measured DOC concentration, lability, and composition, to examine patterns of depletion and production of DOC within the carbon-limited interior of the Nyack aquifer.

2. Study Site

Work was conducted on the Nyack Floodplain, a 16 km^2 montane floodplain on the gravel- and cobble-bedded Middle Fork of the Flathead River, located in northwest Montana, USA (Figure 1a). The river is unmodified and unregulated, and most of the upstream catchment is in federally protected wilderness. Some hay production, cattle grazing, and riparian logging have occurred on the floodplain over the last 100 years, and a railroad and highway traverse the western edge of the floodplain. The river has a snowmelt-driven hydrograph with a mean discharge of 80 $m^3 s^{-1}$ and mean peak discharge of 600 $m^3 s^{-1}$ in the spring [*Poole et al.*, 2004].

The hydrology and geomorphology of the study site are well characterized [*Stanford et al*., 1994; *Poole et al*., 2002, 2004, 2006; *Stanford et al*., 2005; *Whited et al*., 2007; *Helton et al*., 2014]. The river channel flows over bedrock within canyons upstream and downstream of the floodplain, and the floodplain is constrained laterally by bedrock valley walls. The floodplain aquifer is composed of expansive cobble and gravel alluvia varying from 5 to 25 m thick, which overlie a relatively impermeable layer of silt and clay that extends to bedrock. Subsequent flooding and migration of the active river channel have deposited 1 to 3 m of fine sediments on the floodplain surface adjacent to the river [*Stanford et al*., 1994; *Poole et al*., 2002]. Complex channel morphology and coarse, well-sorted sediments on the floodplain facilitate high exchange between the surface and subsurface. The main channel of the river loses ~30–40% of its base flow discharge to the underlying alluvial aquifer as it flows across the upstream third of the study site [*Stanford et al*., 2005; *Helton et al*., 2014]. Bedrock constriction at the downstream end of the floodplain forces this water to reemerge from the alluvial aquifer, back to the main channel, side channels, and spring channels scattered across the downstream half of the study site. Because channel-derived water permeates throughout the cobble and gravel strata and across the entire width of the floodplain (up to 1.5 km) [*Poole et al*., 2004; *Helton et al*., 2014], the alluvial aquifer is essentially an expansive hyporheic zone. Patterns of surface and subsurface exchange are complex and vary seasonally with patterns of floodplain inundation [*Poole et al*., 2006; *Helton et al*., 2014].

3. Methods

3.1. Sample Collection

An existing monitoring well network at the study site includes approximately 50 two or three inch diameter PVC pipes, slotted (every 3.5 cm) below the water table and installed 5 to 8 m into the alluvium. From the network, we selected 12 monitoring wells that span a range of lateral and longitudinal positions within the study site (Figure 1a) and sampled water from each of these wells and from the river channel during nine sampling events between July 2008 and October 2009, which spanned seasons and river discharge conditions (Figure 1b). Within each well, we sampled two depths for a total of 24 aquifer water samples on each date. "Shallow" samples were collected from a depth at or near the base flow water table, and "deep" water samples were collected 2 to 4 m below the shallow sample. The depth of deep water sample collection was constrained by the depth of the well, and samples were collected near the bottom of each well. Surface water sites were located in the river channel at the inlet (upstream) and outlet (downstream) canyons that bound the floodplain.

Immediately prior to collecting water samples from monitoring wells, the entire depth of the well was pumped with a hand-operated diaphragm pump to remove sediments that may have accumulated in the well. Then, rigid tubing with two foam discs, sized to fit snugly within the well, spaced 1 m apart vertically, was inserted into the well to isolate a 1 m sampling interval at the deep sampling depth. A 12 V electric submersible pump (Whale Submersible 881, Whale Systems Specialists) was connected to a flexible tube that extended into the isolated interval between the foam discs. Water was pumped from the isolated interval until dissolved oxygen concentrations (YSI 85; Yellow Springs Instruments) stabilized. Samples were collected from the stream of water flowing from the tube. The discs were then raised to the shallow sampling interval, and the process repeated.

We collected water samples in acid-washed and sample-rinsed polycarbonate or glass bottles. Samples were placed on ice immediately after collection and were stored at 4°C prior to processing. Within 48 h of field collection approximately 200 mL of each sample was filtered through a 0.22 μm nylon membrane filter prerinsed with ~100 mL of distilled deionized water and ~50 mL of sample. When samples could not be immediately analyzed for DOC lability (see below), they were frozen and analyzed within 3 months. A subsample of each filtered sample collected during the 2009 sampling events was immediately preserved with phosphoric acid to pH = 2 for optical measurements (see below).

3.2. DOC Lability Assays

We conducted 3 day DOC lability assays, similar to *Servais et al*. [1989] and *McDowell et al*. [2006], in which we measured initial and final DOC concentrations to estimate microbial consumption of DOC. Assays were conducted at oxygen saturation in a dark environment in 40 mL glass vials. For each assay, we added 25 mL of filtered sample and inoculated this filtered water with 250 μL of unfiltered water, which was prepared by mixing equal volumes of unfiltered well and surface water samples collected within 1 week of incubations.

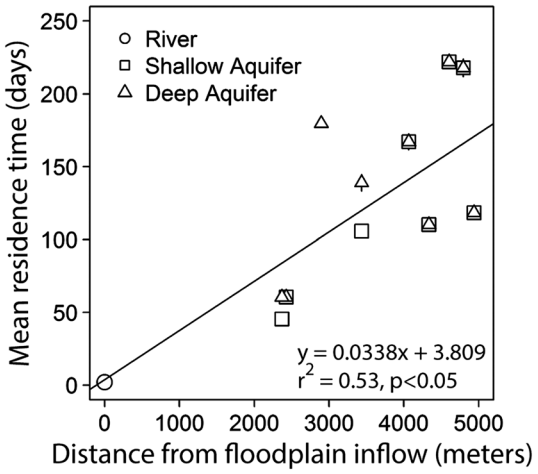

Figure 2. Mean residence time (± se; $n = 9$) simulated by *Helton et al.* [2014] versus distance from river channel at the study site inflow. Symbols cover error bars where error bars are not visible.

Assays were also amended with 50 μL of nutrient solution (0.1% NH_4NO_3 and 0.1% K_2HPO_4), and the vials were capped and incubated in the dark at room temperature (~20°C) for 3 days.

For each sample, we conducted three assays. One assay was inoculated, amended with nutrients, and immediately acidified with 50 μL phosphoric acid to measure initial DOC concentration. Two assays were inoculated and amended with nutrients. We also included two blanks for each sampling event in which inoculate and nutrients were added to 25 mL of distilled water. After 3 days, each assay was acidified with 50 μL phosphoric acid and analyzed for final DOC concentration. Concentrations of DOC were analyzed by combustion [*American Public Health Association*, 1998] on a Tekmar Dohrmann Apollo 9000 TOC system at the Freshwater Research Lab at the University of Montana's Flathead Lake Biological Station.

We calculated labile DOC as DOC depleted (ΔDOC in $\mu g\,L^{-1}$)—the initial DOC ($\mu g\,L^{-1}$) minus the final DOC ($\mu g\,L^{-1}$) concentrations measured in each assay corrected by subtracting initial and final blank DOC concentrations, respectively. Labile DOC reported for each sample is the average calculated from the two assays. We also calculated %ΔDOC by dividing ΔDOC by blank-corrected initial DOC concentration and multiplying by 100.

From the replicate determinations of final DOC concentration for each assay, we calculated the minimum detectable concentration difference (MDCD) between DOC concentrations (i.e., the minimum detectable ΔDOC; modified from *Yates et al.* [2006]). The MDCD was calculated from the following equation for each sampling event:

$$\text{MDCD} = \mu\text{rep diff} + (2\sigma\ \text{rep diff})$$

Where μ is the average difference between replicate final DOC concentrations (rep diff) and σ is the standard deviation of the difference between replicate final DOC concentrations. When ΔDOC was less than MDCD, ΔDOC was considered below detection and was set to ½ MDCD. MDCD varied by less than 10 $\mu g\,L^{-1}$ among sampling events.

To assess the potential effects of freezing on ΔDOC, we analyzed a subset of samples for ΔDOC prefreezing and postfreezing. Freezing did not significantly change measurements of initial or final DOC concentrations ($t = 1.75$; $p > 0.05$; $n = 20$) or estimates of ΔDOC ($t = 1.83$; $p > 0.05$; $n = 10$). All assays conducted with samples postfreezing were inoculated with freshwater from the sampling event closest to the date the assays were conducted. Therefore, the subset of samples analyzed before and after freezing was also inoculated with freshwater collected approximately 2 months apart, which suggests that using inoculum made on different dates was probably not a substantial source of variance in the results.

3.3. Optical Measurements and Analyses

We measured UV-Visible absorbance spectrum between 200 and 700 nm (1 nm increment) using a 1 cm path length quartz cuvette on a Perkin Elmer 559 UV/Visible Spectrophotometer corrected against acidified laboratory grade water blanks. Specific UV absorbance ($SUVA_{254}$), which is strongly correlated with aromatic carbon content, was calculated following *Weishaar et al.* [2003]: measured absorbance at 254 nm was divided by the cuvette path length (in meters) and normalized to DOC concentration ($mg\,L^{-1}$).

Because DOC concentrations are typically low ($<2\ mg\,L^{-1}$), we used a more sensitive technique, fluorescence excitation-emission matrix (EEM) spectroscopy, to explore compositional changes in bulk DOC. Recent studies have used EEMs to characterize the chemical composition of DOC [*Cory et al.*, 2007; *Fellman et al.*, 2010] within a wide range of marine and freshwater environments and to trace changes in DOC production and consumption along environmental gradients and within laboratory experiments [*Cory and Kaplan*, 2012].

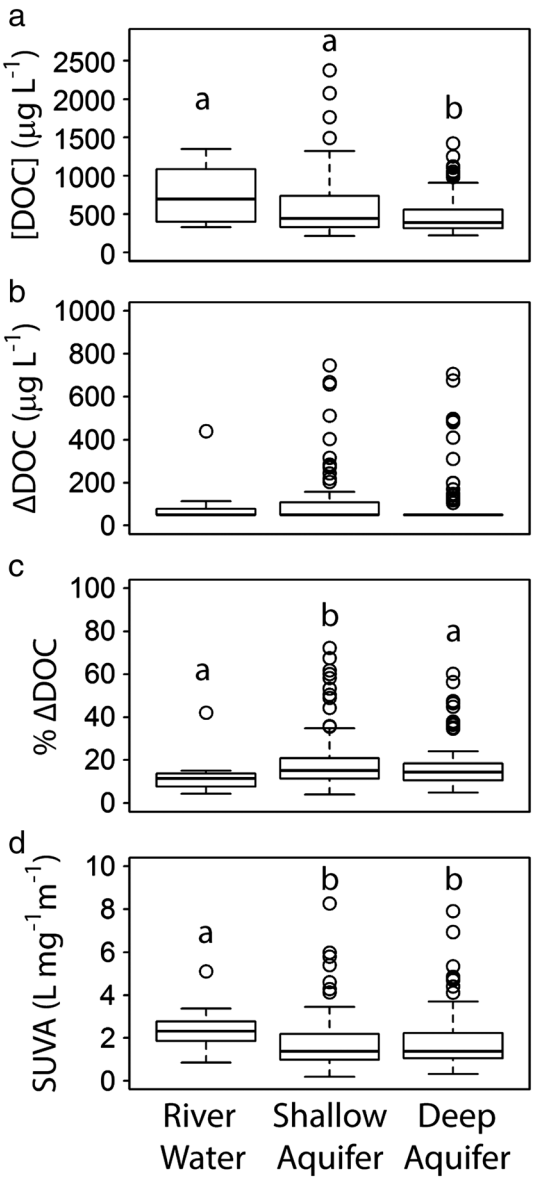

Figure 3. Box plots of (a) DOC concentration, (b) ΔDOC, (c) % ΔDOC, and (d) SUVA for the shallow aquifer, deep aquifer, and river water samples. Boxes show median and interquartile range. Outliers (open circles) are identified as points outside 1.5 times the interquartile range. Letters denote significance at $p<0.05$ from post hoc Tukey HSD.

We measured EEMs in triplicate for acidified DOC water samples collected in 2009 sampling events (April, July, September, and October) using a Fluorolog-3 equipped with a charge-coupled device (CCD) detector (Horiba Jobin Yvon Inc., Edison, NJ). Excitation-emission matrices were created by measuring fluorescence intensity across excitation wavelengths 240 to 450 nm (5 nm increment) and across emission wavelengths 140 to 950 nm (2 nm increment), using a 0.4 s integration time. We corrected EEMs for inner-filter effects and for instrument-specific excitation and emission corrections in MATLAB R2008b (Mathworks) via a user-generated rhodamine spectrum for excitation correction and a manufacturer-provided emission correction spectrum specific to the CCD detector (Horiba Scientific) following *Cory et al*. [2010]. Similarly, analyzed blank EEMs, collected from acidified laboratory grade DI water and free of detectable fluorescence emission, were subtracted from sample EEMs to minimize the influence of water Raman peaks, and intensities in blank-corrected sample EEMs were converted to Raman units [*Stedmon et al*., 2003].

We generated and validated a parallel factor analysis (PARAFAC) model according to *Stedmon and Bro* [2008] using the DOMFluor toolbox in MATLAB R2008b (Mathworks). PARAFAC decomposes EEMs into unique fluorescence groups representing chemically independent components [*Stedmon et al*., 2003]. Because the exact chemical structure of the components is unknown, for each EEM, components are described by F_{max} values, which represent the maximum fluorescence of each component. Prior to PARAFAC, EEM wavelength ranges were reduced to excitation 250 to 450 nm and emission 320 to 550 nm. We removed outlier EEMS and evaluated models with three to six components according to *Stedmon and Bro* [2008]. The number of components was selected based on visual examination of residual EEMs, sum of squared error (SSE), and four-way split-half analysis. Three- and six-component models were not considered because they could not be split-half validated. The five-component model SSE (SSE = 351.6 from random initialization) was not substantially lower than the four-component model (SSE = 371.5 from random initialization), and the four-component model had residual EEMs that mostly contained background noise and explained 99% of the variation in the data set. Component spectra and the validation results for the four-component model are shown in the supporting information Figure S1.

3.4. Hydraulic Residence Time

As a measure of the average hydrologic travel time from the river channel through the aquifer to each sampling location, we used modeled mean hydraulic residence time for each well and sampling depth, as reported by *Helton et al*. [2014]. To calculate mean residence time, *Helton et al*. [2014] implemented a three-dimensional link-and-node hydrologic model for the study site that simulates channel flow, floodplain inundation, and

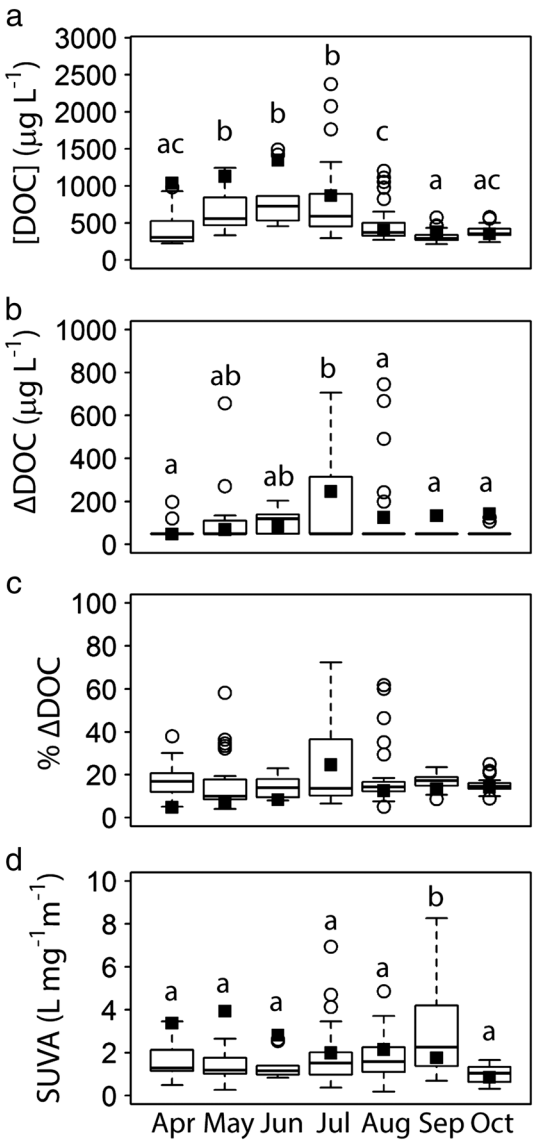

Figure 4. Box plots of (a) DOC concentration, (b) ΔDOC, (c) % ΔDOC, and (d) SUVA grouped by month sampled. Each month was sampled in 2008 and 2009, except April and October, which were only sampled in 2009. Boxes show median and interquartile range. Outliers (open circles) are identified as points outside 1.5 times the interquartile range. Black squares are river water. Letters denote significance at $p<0.05$ from post hoc Tukey HSD.

resulting patterns of aquifer recharge, discharge, and water movement. They developed a particle (e.g., water molecule) tracking postprocessor that tracks conservative tracer particles through the model. The model was run using measured channel discharge in the Middle Fork of the Flathead River from 1996 to 2000, a period that encompassed a range flow conditions (high, intermediate, and low flood years). Mean residence time was calculated as the average time required for a water molecule to traverse the Nyack Floodplain aquifer, from the channel to a sampling location (i.e., a well at a specific depth) over the course of the 5 year hydrologic simulation. Mean residence time yields an overestimate of hydraulic residence time at any given location because particles are forced to travel along modeled links between model nodes, even where links are not perpendicular to isopleths of groundwater head. Thus, mean residence time is a measure of relative, not absolute, residence time.

Analysis of results from the hydrologic simulations provided evidence that the model represented aquifer hydrology and relative mean residence times accurately. The model explained 97 to 99% of variation in observed hydraulic head across 21 sampling wells (including the wells in the current study) [*Helton et al.*, 2014]. Mean residence time also explained observed differences in the phase and amplitude of annual water temperature cycles recorded in 16 monitoring wells distributed across the floodplain ($r^2 = 0.83$ and 0.79 for water temperature amplitude and phase, respectively) [*Helton et al.*, 2012]. Finally, mean residence time increased with longitudinal distance from the upstream bedrock canyon inflow for the wells in the current study (Figure 2), consistent with observations that water recharges the aquifer in the upstream third of the study site, flows through the aquifer, and then reemerges to the surface near the downstream boundary (see section 2 above).

3.5. Data Analysis

All analyses were performed with *R* Statistical Software Version 3.0.2 [*R Core Team*, 2012]. For the full data set, we performed multiple linear regression selection for DOC and ΔDOC using regsubsets() in the leaps package in *R*. Regsubsets() selects the best candidate model for each possible number of parameters, with an exhaustive search that includes every combination of parameters at each level. Dependent variables for the regression analysis included sample depth, residence time, water temperature, air temperature (to account for seasonal differences), and dissolved oxygen. We also used parametric correlations (Pearson product-moment) to address relationships

Table 1. Candidate Multiple Linear Regression Models for DOC and ΔDOC for Each Possible Number of Model Coefficients (*K*), Including the Intercept[a]

Model	*K*	r^2_{adj}	C_p	AIC	Δ_i	RSS
		DOC				
DO	2	0.06	17.18	−482.39	15.10	22.72
DO, Air Temp	3	0.10	6.01	−493.18	4.32	21.42
Air Temp, **RT**, **Water Temp**	**4**	**0.12**	**4.25**	**−497.50**	**0.00**	**21.05**
Air Temp, RT, Water Temp, DO	5	0.12	4.25	−495.02	2.48	20.85
Air Temp, RT, Water Temp, DO, Depth	6	0.12	6.00	−493.27	4.23	20.82
		ΔDOC				
DOC	2	0.59	54.20	−846.82	86.53	3.52
DOC, RT	3	0.65	18.14	−874.62	58.73	3.01
DOC, RT, Water Temp	4	0.66	8.27	−931.48	1.87	2.86
DOC, **RT**, **Water Temp**, **Depth**	**5**	**0.67**	**6.54**	**−933.35**	**0.00**	**2.81**
DOC, RT, WaterTemp, Depth, DO	6	0.67	5.01	−929.78	3.56	2.76
DOC, RT, Water Temp, Depth, DO, Air Temp	7	0.67	7.00	−927.79	5.55	2.76

[a]Reported statistics include adjusted r^2 (r^2_{adj}), Mallows' C_p, Akaike information criterion (AIC), the difference between the candidate and best model's AIC (Δ_i), and the residual sum of squares (RSS). Candidate models with lowest AIC are in bold, and coefficients are reported in Table 2.

between PARAFAC components, DOC, SUVA, and ΔDOC for the full data set. Differences between sample type (river, shallow, and deep aquifer) and sample month were analyzed with one-way analysis of variance (ANOVA) followed by post hoc Tukey's HSD comparisons. Homogeneity of variance among sample months and sample types was tested with the Fligner-Killeen test of homogeneity of variances. Relationships between mean residence time and mean DOC concentration, ΔDOC, %ΔDOC, SUVA, and PARAFAC components were also analyzed with simple linear regression. Data for all analyses were tested for normality with the Shapiro-Wilk normality test. Data were log transformed when necessary to meet assumptions of normality and homogeneity of variance.

4. Results

4.1. Hydraulic Residence Time and Dissolved Oxygen

Simulated mean hydraulic residence time ranged from 45 to 292 days for the wells in this study. Relative to the large difference in residence time between wells, residence time varied little at each sampling location (standard error < 10 days for the nine modeled particle releases across the 5 year simulation). Shallow aquifer sites tended to have lower residence times 138 ± 16 days (mean ± se) than deep aquifer sites 167 ± 22 days (mean ± se), although the difference was not significant ($p = 0.12$).

Dissolved oxygen concentrations were significantly higher in river water (9.8 ± 0.23; mean ± se) than in shallow (4.9 ± 0.25) or deep (5.2 ± 0.26) aquifer water ($F = 17.94$, $p < 0.05$). Averaged dissolved oxygen concentrations decreased with mean residence time for shallow ($y = -0.02x + 7.7$, $r^2 = 0.36$) and deep ($y = -0.02x + 8.0$, $r^2 = 0.37$) aquifer samples ($p < 0.05$).

Table 2. Multiple Linear Regression Coefficient Estimates for Models With Lowest AIC (Table 2 and Supporting Information Table S1)[a]

	DOC			ΔDOC		
Model	All	Shallow	Deep	All	Shallow	Deep
Intercept	0.307	0.252	0.272	**−0.351**	**−0.535**	**−0.212**
DOC	NA	NA	NA	**0.497**	**0.595**	**0.367**
RT	**−0.00123**	**−0.00076**	**−0.00061**	**0.000930**	**0.00150**	**0.000445**
Air Temp	**0.0111**	**0.0126**	**0.00838**			
Water Temp	**−0.0275**		**−0.0205**	**0.0113**	**0.0147**	0.00591
Depth		NA	NA	−0.00290	NA	NA
DO		**0.0400**				
p	<0.001	0.001	0.01	<0.001	<0.001	<0.001
n	216	108	108	216	108	108

[a]Bold coefficients have $p < 0.05$. NA: not available.

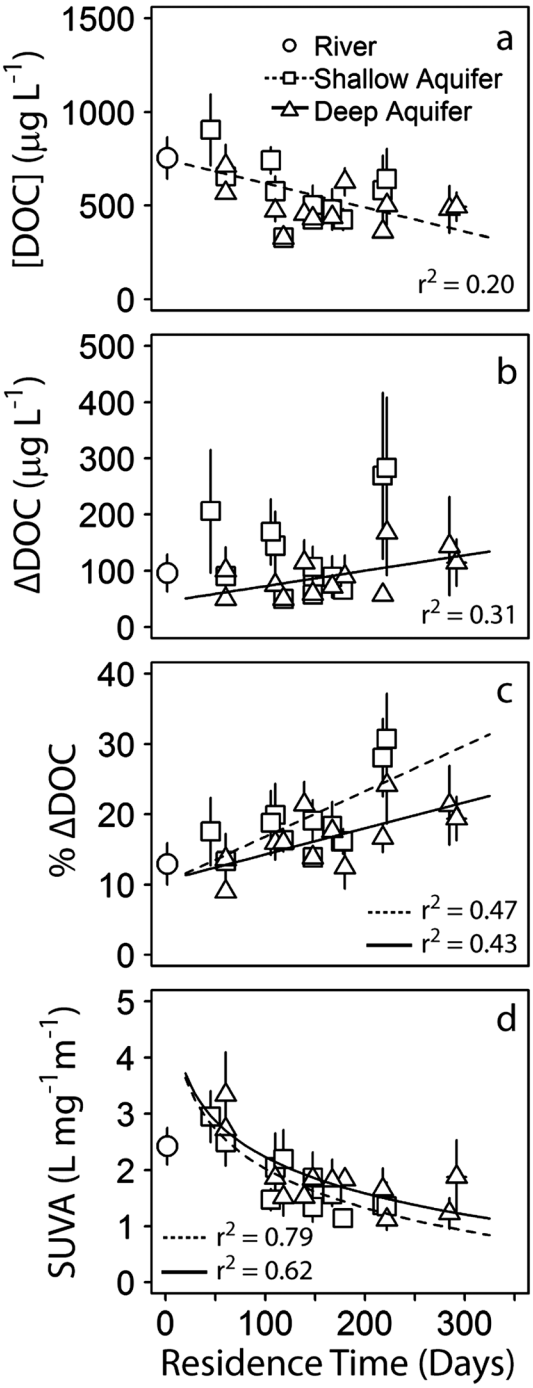

Figure 5. Mean dissolved organic carbon metrics averaged across sampling dates (± se; $n = 9$) versus mean hydraulic residence time (± se; $n = 9$) for (a) DOC concentration, (b) ΔDOC, (c) percent of ΔDOC, and (d) SUVA. Circles are river water. All regressions shown are significant at $p < 0.05$. Symbols cover error bars where error bars are not visible.

4.2. Patterns of DOC Concentration

Concentrations of DOC were typically low, averaging 542 ± 22.7 μg L^{-1} (mean ± se) with minimum and maximum values of 212 and 2375 μg L^{-1}. Concentrations of DOC in river water (755 ± 112 μg L^{-1}) tended to be higher than DOC in the shallow aquifer (548 ± 39.5 μg L^{-1}) and were significantly higher than DOC in the deep aquifer (488 ± 24.1) ($F = 4.507$; $p < 0.05$) (Figure 3a). Concentrations of DOC changed significantly with sampling month ($F = 14.8$; $p < 0.05$) and were highest and most variable in May, June, and July and lowest and least variable in September and October (Figure 4a). River water DOC concentrations followed the same temporal trends as aquifer water DOC concentrations, with higher concentrations in spring and summer months and lower concentrations in fall months (Figure 4a, black squares). River water DOC tended to be higher than aquifer DOC concentrations in spring and summer months but more similar to aquifer DOC concentrations in fall months (Figure 4a).

The multiple linear regression analysis explained 12% of variation in DOC concentration across the whole data set (Table 1). The best model included a positive regression coefficient for air temperature (Table 2), confirming the seasonal pattern in Figure 4a that shows higher DOC concentrations during spring and summer months. The best model also included significant negative regression coefficients for water temperature and residence time (Table 2), suggesting lower DOC in cooler water and farther along aquifer flow paths. Regression coefficients for air temperature and residence time of best models were similar for shallow and deep aquifer samples (Table 2 and supporting information Table S1), but the best model for the deep aquifer samples explained only 8% of variation in the data set (Table S1). Indeed, average DOC concentrations decreased significantly with mean residence time for the shallow but not for the deep aquifer water samples (Figure 5a).

4.3. Patterns of DOC Lability

Lability of DOC (ΔDOC) averaged 117 ± 13.5 μg L^{-1} (mean ± se), with the proportion of labile DOC varying considerably from as low as 4% to as high as 72% of total DOC across all samples. Annual average concentrations of shallow aquifer ΔDOC (147 ± 26.2 μg L^{-1}), deep aquifer ΔDOC (92.7 ± 12.0 μg L^{-1}), and river water ΔDOC (96.2 ± 33.6 μg L^{-1}) were not significantly different from one another ($F = 2.048$; $p = 0.13$) (Figure 3b). However, the majority of high ΔDOC values was measured in the shallow and deep aquifer, with only one value above 200 μg L^{-1} measured in river water (Figure 3b). Seasonal patterns of ΔDOC followed similar patterns to DOC concentrations and were significantly different among sampling

Table 3. Characteristics of the Four PARAFAC Components Identified in This Study Compared With Those Previously Identified

Component	Ex. Max.	Em. Max.	Description	References
1	<250 (350)	476	Terrestrial, humic like	P3(<260,380/498): *Murphy et al.* [2008]; C2 (<250, 385/504): *Stedmon and Markager* [2005]; and C (350/420-480): *Coble* [1996]
2	<250 (320)	399	Autochthonous and terrestrial, humic like	P1 (<260,310/414): *Murphy et al.* [2008]; C3 (<250, 305/412) and C4 (<250, 360/440): *Stedmon and Markager* [2005]; and A (260/380–460) and M (312/380–420): *Coble* [1996]
3	275	322	Autochthonous, amino acid like (tyrosine like)	AK9 (270/306): *Fellman et al.* [2009]; P5 (270/310), P6 (275/318): *Murphy et al.* [2008]; C13 (280/<350): *Cory and McKnight* [2005]; C8 (275/304): *Stedmon and Markager* [2005]; and B (275/310): *Coble* [1996]
4	<250 (290)	342	Autochthonous, amino acid like (tryptophan like)	AK10 (280/336): *Fellman et al.* [2009]; P7 (280/342): *Murphy et al.* [2008]; C8 (270/<350): *Cory and McKnight* [2005]; C7 (280/344): *Stedmon and Markager* [2005]; and T (275/340): *Coble* [1996]

months ($F = 7.489$; $p < 0.05$). Average ΔDOC concentrations increased from April to July, were highest and most variable in July, and remained typically near or below detection in September and October (Figure 4b). Surface water ΔDOC concentrations followed the same temporal trends as aquifer water ΔDOC concentrations, with highest lability in July (Figure 4b, black squares).

Percent ΔDOC (%ΔDOC) was strongly correlated to ΔDOC ($r = 0.87$), and they showed similar spatial and temporal patterns. On average, 18 ± 12% of the bulk DOC was bioavailable (%ΔDOC). This labile fraction tended to be higher in the shallow aquifer (19.7 ± 1.4%) and was significantly higher in the deep aquifer (17.1 ± 1.0%) than in the river water (12.9 ± 3.0%) ($F = 3.301$; $p < 0.05$) (Figure 3c). Similar to ΔDOC, the majority of high %ΔDOC values was measured in the aquifer, with only one value above 20% measured in the river water (Figure 3c). Percent ΔDOC did not change significantly with sampling month ($F = 1.717$; $p = 0.12$) but tended to follow patterns similar to ΔDOC, with highest and most variable values in July (Figure 4c).

A multiple-regression model including DOC concentration, water residence time, water temperature, and sampling depth explained 67% of variation in ΔDOC and had the lowest AIC (Tables 1 and 2). Dissolved organic carbon was included in best models at all parameter levels and explained 59% of variation alone (Table 1). Model coefficients were significant and positive for residence time and water temperature, suggesting that both higher temperatures and longer residence times lead to higher ΔDOC. Regression coefficients of best models were similar for shallow and deep aquifer samples (Table 2 and supporting information Table S1).

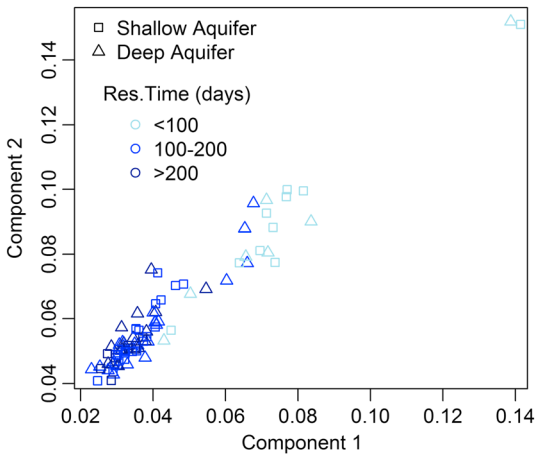

Figure 6. F_{max} values for humic-like PARAFAC components, component 2 versus component 1.

On average, higher ΔDOC values were measured at wells with higher residence times, and ΔDOC significantly increased with residence time within samples collected from the deep aquifer (Figure 5b). Although regression coefficients for ΔDOC were similar for shallow and deep samples (Table 2), two sampling locations with residence times > 200 days appear to drive this relationship for the shallow aquifer samples (Figure 5b). If data from these two locations are removed from the relationship, then average ΔDOC decreases with residence time for shallow aquifer samples with residence time < 200 days ($r^2 = 0.38$; $p < 0.05$). However, on average, %ΔDOC significantly increased with aquifer residence time within samples from both the shallow and deep aquifer (Figure 5c).

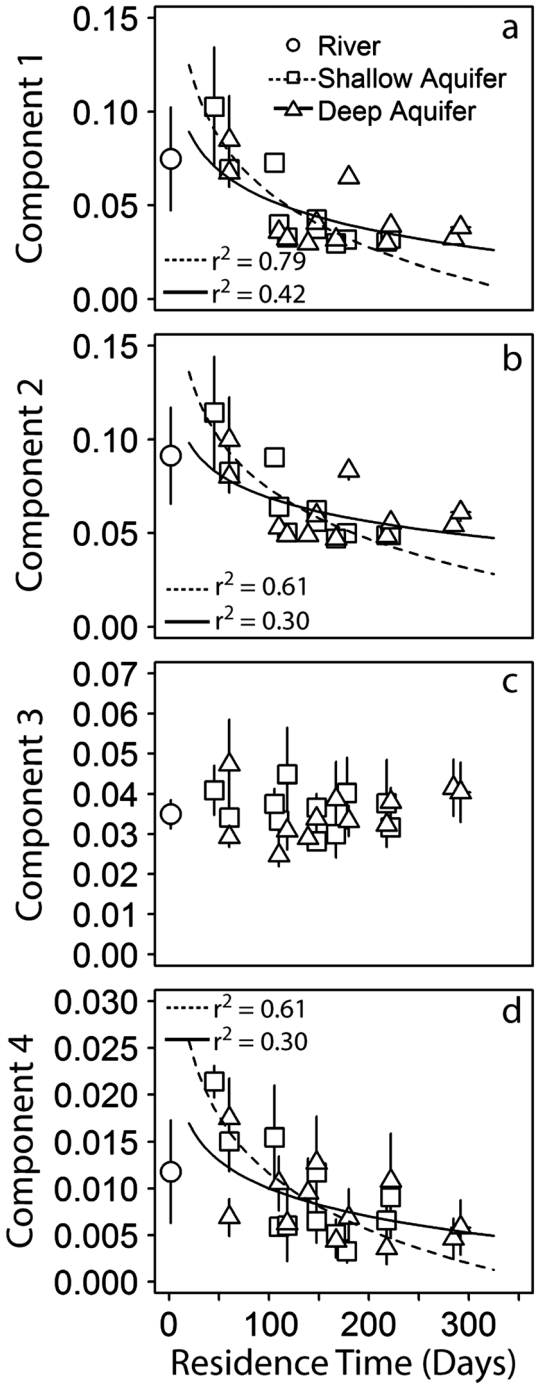

Figure 7. Mean F_{max} values averaged across sampling dates (± se; $n = 5$) for PARAFAC model components (a) 1, (b) 2, (c) 3, and (d) 4 versus mean hydraulic residence time (± se; $n = 9$). All regressions shown are significant at $p < 0.05$. Symbols cover error bars where error bars are not visible.

4.4. Patterns of DOC Composition

Values of SUVA averaged 1.8 ± 0.09 L mg^{-1} cm^{-1} (mean ± se). River water SUVA (2.4 ± 0.30) was significantly higher than both shallow (1.8 ± 0.13) and deep (1.8 ± 0.12) aquifer SUVA ($F = 2.24$; $p < 0.05$) (Figure 3d). Values of SUVA changed significantly with sampling month ($F = 7.08$, $p < 0.05$), with higher SUVA in September than all other months (Figure 4d). On average, SUVA strongly decreased with residence time in both the shallow and deep aquifer (Figure 5d).

Comparing the components in our PARAFAC model to previously published models, we interpret component 1 (C1) and component 2 (C2) as possessing fluorescence characteristics typical of humic organic matter and component 3 (C3) and component 4 (C4) as possessing fluorescence characteristics similar to amino acids (Table 3). Component 1 ($r = 0.66$), C2 ($r = 0.70$), and C4 ($r = 0.45$) ($p < 0.05$) each increased with DOC concentration, and C1 ($r = 0.28$), C2 ($r = 0.26$), and C4 (0.39) ($p < 0.05$) also increased with SUVA. Components were not significantly correlated to ΔDOC.

Humic-like components (C1 and C2) were strongly correlated with one another across the full data set ($r = 0.98$; $p < 0.05$). Humic-like components showed a clear decreasing trend with residence time across the full data set (Figure 6) and on average (Figures 7a and 7b), suggesting that wells with higher residence times were depleted of humic-like dissolved organic matter. While one of the amino acid-like components (C4) was also correlated to C1 ($r = 0.44$) and C2 ($r = 0.46$) ($p < 0.05$), and decreased on average with residence time (Figure 7d), amino acid-like components showed stronger and more consistent trends with sampling month, with significantly higher values in summer than fall or spring months (Table 4). For C3 in the deep aquifer samples (Figure 7c), removing one outlier sample at the shortest residence time well yields a strong positive correlation, with average C3 increasing with residence time ($r^2 = 0.62$; $p < 0.05$).

5. Discussion

Similar to other studies of carbon cycling in the hyporheos, we measured declines in DOC concentrations with water residence time in the Nyack aquifer. In strong contrast to the majority of work to date, we also measured a substantial accumulation of labile DOC within the aquifer interior. This surprising finding provides strong support for nonriverine influx or internal production of DOC as an important contributor to aquifer food webs and carbon cycling. We are not currently able to distinguish the sources of this labile carbon, but below we discuss the evidence that support several potential sources, including

Table 4. Mean ± Standard Error of F_{max} Values for PARAFAC Components and ANOVA Results (*F* Statistics Reported Where $p < 0.05$)[a]

PARAFAC Component	Apr	Jul	Sep	Oct	*F* Statistic
C1	0.052 ± 0.008	0.046 ± 0.003	0.041 ± 0.003	0.040 ± 0.002	ns
C2	0.071 ± 0.007	0.067 ± 0.003	0.056 ± 0.003	0.056 ± 0.002	ns
C3	0.037 ± 0.004[a]	0.041 ± 0.003[ab]	0.033 ± 0.001[a]	0.029 ± 0.002[ac]	3.64
C4	0.010 ± 0.001[a]	0.016 ± 0.001[b]	0.0045 ± 0.001[c]	0.0042 ± 0.001[c]	15.21

[a]Letters denote significance at $p<0.05$ from post hoc Tukey HSD.

leaching from floodplain soils, legacy deposits of buried organic matter, and methanotrophy, which may be contributing energy to fuel these subsurface ecosystems.

5.1. DOC Quantity Versus Quality

Our results provide evidence that water flux through the aquifer had contrasting effects on DOC quantity and DOC quality. Patterns of DOC and labile DOC depletion along hyporheic flow paths have been described in numerous previous studies within small streams [e.g., *Findlay et al*., 1993; *Hedin et al*., 1998; *Baker et al*., 1999] or along the first few meters of aquifer flow paths [*Marmonier et al*., 1995]. Biological consumption of DOC [*Sobczak and Findlay*, 2002] as well as physical sorption of DOC to mineral surfaces [*McKnight et al*., 1992; *Findlay and Sobczak*, 1996; *Fiebig*, 1997] or groundwater dilution [*Lapworth et al*., 2009; *Foulquier et al*., 2010] may contribute to DOC declines along hyporheic flow paths. In the larger alluvial aquifer in this study, we likewise found that DOC concentrations and dissolved oxygen concentrations decreased with residence time [see also *Helton et al*., 2012], suggesting that some DOC is consumed by microbes as water is transported along flow paths. However, we observed the opposite pattern for labile DOC. Labile DOC increased with water residence time, in terms of mass and as a percentage of DOC. There is some precedent for this finding in the literature, as a recent analysis of the Yukon River showed that deeper groundwater flow paths can contribute highly labile DOC during base flows [*Wickland et al*., 2012]. However, our results contrast with the majority of studies along the first few meters of flow paths that show high-quality DOC is degraded first, leaving more recalcitrant DOC downstream.

Optical properties shed additional light on DOC assay results. Because amino acids are strongly related to the lability of DOC (e.g., *Fellman et al*. [2009], but see *Cory and Kaplan* [2012]), declines in amino acid-like component 4 with residence time suggest some biological processing of DOC within the aquifer. However, declines in metrics indicative of more recalcitrant DOC were more strongly related to residence time (SUVA and both humic-like PARAFAC components). This preferential loss of aromatic DOC (i.e., SUVA) and humic-like DOC is consistent with the well-understood process of DOC sorption to sediments [*Marmonier et al*., 1995] and suggests that sorption may play a substantial role in the removal of DOC in the aquifer. Overall, the lability assay results combined with the PARAFAC results suggest a net depletion of lower quality humic-like DOC with concurrent influx and/or production of more labile DOC as water parcels move through the Nyack alluvial aquifer.

5.2. Environmental Conditions for Labile DOC Accumulation

Since the Nyack aquifer has relatively low DOC concentrations, our finding that labile DOC increases with hydraulic residence time is somewhat surprising given that we would expect strong competition for labile DOC along a carbon-limited aquifer flow path. The differences between laboratory and in situ conditions may provide an explanation: Along the gradient of hydraulic residence times, in situ temperatures tend to decrease (during summer sampling events), dissolved oxygen decreases, and microbial biomass likely decreases [*Ellis et al*., 1998]. We conducted laboratory assays at ~20°C (much warmer than in situ conditions) and fully saturated dissolved oxygen concentrations (typically higher than in situ conditions) and inoculated with equal microbial biomass. Thus, the laboratory assays optimized conditions for oxic consumption of labile carbon—conditions that are not likely to occur kilometers along flow paths in the aquifer. Thus, we expect that far less of the DOC pool would be consumed under ambient field conditions where microbial uptake may be limited by temperature and/or oxygen, which would allow labile forms to accumulate along longer flow paths.

5.3. Leaching of Carbon From Floodplain Soils

Leaching from terrestrial soils can be a substantial carbon source to the hyporheic zone in many floodplains [*Clinton et al*., 2002]. Humic-like components and SUVA decreased with residence time within the Nyack

aquifer, suggesting that carbon compounds typically associated with terrestrially derived carbon likely decreased with increasing aquifer residence time. However, because more aromatic DOC sorbs to soils, vertically leached DOC to the alluvial aquifer may have lower than expected aromatic content [e.g., *Qualls and Haines*, 1992]. If the terrestrial ecosystem is responsible for contributing labile DOC, we would expect labile DOC concentrations to be higher near the water table than deeper within sampling wells. Although sampling depth was not a particularly important explanatory variable in the best model for ΔDOC, we did find that DOC concentration and % ΔDOC were significantly higher in the shallow aquifer than the deep aquifer (Figure 3). This suggests that soils near the water table may provide some additional sources of DOC to the shallow aquifer. Because the spatial distribution of floodplain forest regeneration and associated soil development is tightly linked to large flood disturbances that reconfigure surface water channels [*Whited et al*., 2007], wells farther from the river channel (which also tend to have longer residence times) may experience more leaching from more developed soils. In addition, previous research from the Nyack reports high rates of exchange of dissolved oxygen between the vadose zone and the aquifer [*Smith et al*., 2011], further supporting the potential significant exchange of dissolved solutes between floodplain soils and the saturated aquifer.

5.4. Sources of Labile Carbon Within the Aquifer

Although DOC and %ΔDOC were typically higher for samples from the shallow aquifer, the mass of ΔDOC increased with residence time for samples from the deep aquifer, suggesting some additional source or influx of carbon from within the deeper aquifer. In situ conditions within the Nyack aquifer, including low DOC ($<2\,mg\,L^{-1}$) and high DIC ($\sim30\,mg\,L^{-1}$), are conducive to substantial microbial carbon production via chemoautotrophic or methanotrophic pathways, which may represent another important bioavailable DOC source within the aquifer. Biogenic methane as a carbon and energy source has been recognized for its widespread importance in lakes, with methane-derived carbon contributing as much as 70% of invertebrate biomass (reviewed by *Jones and Grey* [2010]). Methane-derived carbon can also provide large carbon subsidies for small streams [*Kohzu et al*., 2004; *Deines et al*., 2007; *Trimmer et al*., 2009] and in gravel beds of large rivers (e.g., up to 46% of net photosynthetic production [*Shelley et al*., 2014]). In fact, in the Nyack aquifer measurements of high concentrations of dissolved methane in well water samples (up to $170\,\mu mol\,L^{-1}$, A. DelVecchia, Flathead Lake Biological Station, unpublished data, 2015) and highly depleted ^{13}C within the body mass of hyporheic invertebrates [*Reid*, 2007] suggest that methanogenesis and methane assimilation may be important carbon pathways within this aquifer.

Although the soil, vadose zone, and stream sediments act as strong filters for POM, large pools of POM are often observed in the subsurface of alluvial river floodplains [*Gurwick et al*., 2008; *Appling et al*., 2014]. Invertebrate abundance tends to increase with organic matter content in interstitial habitats [*Williams and Hynes*, 1974; *Strayer et al*., 1997; *Crenshaw et al*., 2002], and the breakdown of stored POM can increase labile DOC within stream and floodplain subsurface environments [*Crocker and Meyer*, 1987; *Schindler and Krabbenhoft*, 1998; *Gurwick et al*., 2008]. Numerous organic deposits have been identified within the Nyack aquifer, directly through the excavation of soil pits [*Appling et al*., 2014] and indirectly through measurements of distinct areas of low dissolved oxygen that may be indicative of areas of high microbial activity caused by coarse POM buried in the aquifer [*Reid*, 2007; *Valett et al*., 2014]. In fact, *Appling et al*. [2014] estimate that the aquifer contains nearly 37×10^3 Mg of buried particulate carbon, an amount equivalent to the upper meter of floodplain soil. Thus, the breakdown of POM and biogenic methane are potential explanations for the increase in DOC lability within the aquifer interior.

6. Conclusions

Although total DOC declined, DOC lability increased with hydraulic residence time within the aquifer. Aromatic and humic-like DOC decreased, consistent with sorption to aquifer sediments, while labile DOC increased, particularly in the deeper aquifer. Our results suggest that DOC dynamics in this alluvial aquifer are far more complex than a simple depletion of riverine carbon along subsurface flow paths. Mechanisms including leaching from floodplain soils, the storage and mineralization of particulate organic matter, and the microbial production and consumption of methane likely act together to control carbon cycling within this alluvial river aquifer.

Acknowledgments

Data from this paper are available from the first author by request. This research was supported by the Gordon and Betty Moore Foundation for A.M.H., M.S.W., E.S.B., G.C.P., and J.A.S.; by an EPA Star Fellowship for A.M.H.; and by the Odum School of Ecology for A.M.H. EPA has not officially endorsed this publication, and the views expressed herein may not reflect the views of the EPA. We thank Oriana Grubisic, Rachel Malison, and Tyler Tappenbeck for field assistance and Kristin Olson and Katie Harrold for laboratory assistance. We thank the Dalimata family for allowing us to sample on their property. This manuscript was improved by reviews from John Davis, Cynthia Tant, Andrew Mehring, Maury Valett, and three anonymous reviewers.

References

American Public Health Association (APHA) (1998), *Standard Method for Examination of Water and Wastewater*, Am. Public Health Assoc. Publ., APHA, AWWA, WEF, Washington, D. C.

Appling, A. P., E. S. Bernhardt, and J. A. Stanford (2014), Floodplain biogeochemical mosaics: A multidimensional view of alluvial soils, *J. Geophys. Res. Biogeosci.*, *119*, 1538–1553, doi:10.1002/2013JG002543.

Baker, M. A., C. N. Dahm, and H. M. Valett (1999), Acetate retention and metabolism in the hyporheic zone of a mountain stream, *Limnol. Oceanogr.*, *44*, 1530–1539, doi:10.4319/lo.1999.44.6.1530.

Bencala, K. E., M. N. Gooseff, and B. A. Kimball (2011), Rethinking hyporheic flow and transient storage to advance understanding of stream-catchment connections, *Water Resour. Res.*, *47*, W00H03, doi:10.1029/2010WR010066.

Boulton, A. J. (2000), The subsurface macrofauna, in *Streams and Ground Waters*, edited by J. B. Jones and P. J. Mulholland, pp. 337–361, Elsevier, San Diego, Calif.

Clinton, S. M., R. T. Edwards, and R. J. Naiman (2002), Forest-river interactions: Influence on hyporheic dissolved organic carbon concentrations in a floodplain terrace, *J. Am. Water Resour. Assoc.*, *38*, 619–631, doi:10.1111/j.1752-1688.2002.tb00984.x.

Coble, P. G. (1996), Characterization of marine and terrestrial DOM in seawater using excitation emission matrix spectroscopy, *Mar. Chem.*, *51*, 325–346, doi:10.1016/0304-4203(95)00062-3.

Cory, R. M., and D. M. McKnight (2005), Fluorescence spectroscopy reveals ubiquitous presence of oxidized and reduced quinones in dissolved organic matter, *Environ. Sci. Technol.*, *39*, 8142–8149, doi:10.1021/es0506962.

Cory, R. M., and L. A. Kaplan (2012), Biological lability of streamwater fluorescent dissolved organic matter, *Limnol. Oceanogr.*, *57*(5), 1347–1380, doi:10.4319/lo.2012.57.5.1347.

Cory, R. M., D. M. McKnight, Y. Chin, P. Miller, and C. Jaros (2007), Chemical characteristics of fulvic acids from Arctic surface waters: Microbial contributions and photochemical transformations, *J. Geophys. Res.*, *112*, G04S51, doi:10.1029/2006JG000343.

Cory, R. M., M. P. Miller, D. M. McKnight, J. J. Guerard, and P. L. Miller (2010), Effect of instrument response on the analysis of fulvic acid fluorescence spectra, *Limnol. Oceanogr. Methods*, *8*, 67–78, doi:10.4319/lom.2010.8.67.

Craft, J. A., J. A. Stanford, and M. Pusch (2002), Microbial respiration within a floodplain aquifer of a large gravel-bed river, *Freshwater Biol.*, *47*, 251–261, doi:10.1046/j.1365-2427.2002.00803.x.

Crenshaw, C. A., H. M. Valett, and J. L. Tank (2002), Effects of coarse particulate organic matter on fungal biomass and invertebrate density in the subsurface of a headwater stream, *J. North Am. Benthol. Soc.*, *21*, 28–42.

Crocker, M. T., and J. L. Meyer (1987), Interstitial dissolved organic carbon in sediments of a southern Appalachian headwater stream, *J. North Am. Benthol. Soc.*, *6*, 159–167, doi:10.2307/1467507.

Danielopol, D. L. (1989), Groundwater fauna associated with riverine aquifers, *J. North Am. Benthol. Soc.*, *8*, 18–35, doi:10.2307/1467399.

Datry, T., F. Malard, and J. Gibert (2005), Response of invertebrate assemblages to increased groundwater recharge rates in a phreatic aquifer, *J. North Am. Benthol. Soc.*, *24*(3), 461–477, doi:10.1899/0887-3593(2005)024\[0461:ROIATI\]2.0.CO;2.

Deines, P., J. Grey, H. H. Richnow, and G. Eller (2007), Linking larval chironomids to methane: Seasonal variation of the microbial methane cycle and chironomid delta C-13, *Aquat. Microb. Ecol.*, *46*, 273–282.

Ellis, B. K., J. A. Stanford, and J. V. Ward (1998), Microbial assemblages and production in alluvial aquifers of the Flathead River, Montana, USA, *J. North Am. Benthol. Soc.*, *17*, 382–402, doi:10.2307/1468361.

Fellman, J. B., E. Hood, D. V. D'Amore, R. T. Edwards, and D. White (2009), Seasonal changes in the chemical quality and biodegradability of dissolved organic matter exported from soils to streams in coastal temperate rainforest watersheds, *Biogeochemistry*, *95*, 277–293, doi:10.1007/s10533-009-9336-6.

Fellman, J. B., E. Hood, and R. G. M. Spencer (2010), Fluorescence spectroscopy opens new windows into dissolved organic matter dynamics in freshwater ecosystems: A review, *Limnol. Oceanogr.*, *55*, 2452–2462, doi:10.4319/lo.2010.55.6.2452.

Fiebig, D. M. (1997), Microbiological turnover of amino acids immobilized from groundwater discharged through hyporheic sediments, *Limnol. Oceanogr.*, *42*, 763–768, doi:10.4319/lo.1997.42.4.0763.

Findlay, S., and W. V. Sobczak (1996), Variability in removal of dissolved organic carbon in hyporheic sediments, *J. North Am. Benthol. Soc.*, *15*, 35–41, doi:10.2307/1467431.

Findlay, S., D. Strayer, C. Goumbala, and K. Gould (1993), Metabolism of streamwater dissolved organic-carbon in the shallow hyporheic zone, *Limnol. Oceanogr.*, *38*, 1493–1499.

Foulquier, A., F. Malard, F. Mermillod-Blondin, T. Datry, L. Simon, B. Montuelle, and J. Gibert (2010), Vertical change in dissolved organic carbon and oxygen at the water table region of an aquifer recharged with stormwater: Biological uptake or mixing?, *Biogeochemistry*, *99*, 31–47, doi:10.1007/s10533-009-9388-7.

Gibert, J., and L. Deharveng (2002), Subterranean ecosystems: A truncated functional diversity, *BioScience*, *52*(6), 473–481, doi:10.1641/0006-3568(2002)052[0473:SEATFB]2.0.CO;2.

Gurwick, N. P., P. M. Groffman, J. B. Yavitta, A. J. Gold, G. Blazejewskid, and M. Stolt (2008), Microbially available carbon in buried riparian soils in a glaciated landscape, *Soil Biol. Biochem.*, *40*, 85–96, doi:10.1016/j.soilbio.2007.07.007.

Hedin, L. O., J. C. von Fischer, N. E. Ostrom, B. P. Kennedy, M. G. Brown, and G. P. Robertson (1998), Thermodynamic constraints on nitrogen transformations and other biogeochemical processes at soil-stream interfaces, *Ecology*, *79*, 684–703, doi:10.1890/0012-9658(1998)079[0684:TCONAO]2.0.CO;2.

Helton, A. M., G. C. Poole, R. A. Payn, C. Izurieta, and J. A. Stanford (2012), Scaling flow path processes to fluvial landscapes: An integrated field and model assessment of temperature and dissolved oxygen dynamics in a river-floodplain-aquifer system, *J. Geophys. Res.*, *117*, G00N14, doi:10.1029/2012JG002025.

Helton, A. M., G. C. Poole, R. A. Payn, C. Izurieta, and J. A. Stanford (2014), Relative influences of the river channel, floodplain surface, and alluvial aquifer on simulated hydrologic residence time in a montane river floodplain, *Geomorphology*, doi:10.1016/j.geomorph.2012.01.004.

Jones, R. I., and J. Grey (2010), Biogenic methane in freshwater food webs, *Freshwater Biol.*, *56*, 213–299, doi:10.1111/j.1365-2427.2010.02494.x.

Kohzu, A., C. Kato, T. Iwata, D. Kishi, M. Murakami, S. Nakano, and E. Wada (2004), Stream food web fueled by methane-derived carbon, *Aquat. Microb. Ecol.*, *36*, 189–194.

Lapworth, D. J., D. C. Gooddy, D. Allen, and G. H. Old (2009), Understanding groundwater, surface water, and hyporheic zone biogeochemical processes in a Chalk catchment using fluorescence properties of dissolved and colloidal organic matter, *J. Geophys. Res.*, *114*, G00F02, doi:10.1029/2009JG000921.

Marmonier, P., D. Fontvieille, J. Gibert, and V. Vanek (1995), Distribution of dissolved organic-carbon and bacteria at the interface between the Rhone River and its alluvial aquifer, *J. North Am. Benthol. Soc.*, *14*, 382–392, doi:10.2307/1467204.

McDowell, W. H., A. Zsolnay, J. A. Aitkenhead-Peterson, E. G. Gregorich, D. L. Jones, D. Jodemann, K. Kalbitz, B. Marschner, and D. Schwesig (2006), A comparison of methods to determine the biodegradable dissolved organic carbon from different terrestrial sources, *Soil Biol. Biochem.*, *38*, 1933–1942, doi:10.1016/j.soilbio.2005.12.018.

McKnight, D. M., K. E. Bencala, G. W. Zellweger, G. R. Aiken, G. L. Feder, and K. A. Thorn (1992), Sorption of dissolved organic carbon by hydrous aluminum and iron oxides occurring at the confluence of Deer Creek with the Snake River, Summit County, Colorado, *Environ. Sci. Technol.*, *26*, 1388–1396, doi:10.1021/es00031a017.

Miller, M. P., D. M. McKnight, R. M. Cory, M. W. Williams, and R. L. Runkel (2006), Hyporheic exchange and fulvic acid redox reactions in an alpine stream/wetland ecosystem, Colorado Front Range, *Environ. Sci. Technol.*, *40*, 5943–5949, doi:10.1021/es060635j.

Murphy, K. R., C. A. Stedmon, T. D. Waite, and G. M. Ruiz (2008), Distinguishing between terrestrial and autochthonous organic matter sources in marine environments using fluorescence spectroscopy, *Mar. Chem.*, *108*, 40–58, doi:10.1016/j.marchem.2007.10.003.

Poole, G. C., J. A. Stanford, C. A. Frissell, and S. W. Running (2002), Three-dimensional mapping of geomorphic controls on flood-plain hydrology and connectivity from aerial photos, *Geomorphology*, *48*(4), 329–347, doi:10.1016/S0169-555X(02)00078-8.

Poole, G. C., J. A. Stanford, S. W. Running, C. A. Frissell, W. W. Woessner, and B. K. Ellis (2004), A patch hierarchy approach to modeling surface and subsurface hydrology in complex flood-plain environments, *Earth Surf. Processes Landforms*, *29*, 1259–1274, doi:10.1002/esp.1091.

Poole, G. C., J. A. Stanford, S. W. Running, and C. A. Frissell (2006), Multiscale geomorphic drivers of groundwater flow paths: Subsurface hydrologic dynamics and hyporheic habitat diversity, *J. North Am. Benthol. Soc.*, *25*, 288–303, doi:10.1899/0887-3593(2006)25[288:MGDOGF]2.0.CO;2.

Poole, G. C., S. J. O'Daniel, K. L. Jones, W. W. Woessner, E. S. Bernhardt, A. M. Helton, J. A. Stanford, B. R. Boer, and T. J. Beechie (2008), Hydrologic spiralling: The role of multiple interactive flow paths in stream ecosystems, *River Res. Appl.*, *24*, 1018–1031, doi:10.1002/rra.1099.

Qualls, R. G., and B. L. Haines (1992), Biodegradability of dissolved organic matter in forest throughfall, soil solution and stream water, *Soil Sci. Soc. Am. J.*, *56*, 578–586, doi:10.2136/sssaj1992.03615995005600020038x.

R Core Team (2012), *R: A Language and Environment for Statistical Computing*, R Foundation for Statistical Computing, Vienna. [Available at http://www.R-project.org/.]

Reid, B. L. (2007), Energy flow in a floodplain aquifer ecosystem, PhD dissertation, Univ. of Montana, Missoula.

Reynolds, S. K., and A. C. Benke (2012), Chironomid production along a hyporheic gradient in contrasting stream types, *Freshwater Sci.*, *3*, 167–181, doi:10.1899/11-017.1.

Schindler, J. E., and D. P. Krabbenhoft (1998), The hyporheic zone as a source of dissolved organic carbon and carbon gases to a temperate forested stream, *Biogeochemistry*, *43*, 157–174, doi:10.1023/A:1006005311257.

Servais, P., A. Anzil, and C. Ventresque (1989), Simple method for determination of biodegradable dissolved organic carbon in water, *Appl. Environ. Microbiol.*, *55*, 2732–2734.

Shelley, F., J. Grey, and M. Trimmer (2014), Widespread methanotrophic production in lowland chalk rivers, *Proc. Biol. Sci.*, *281*(1783), 20132854, doi:10.1098/rspb.2013.2854.

Smith, M. G., S. R. Parker, C. H. Gammons, S. R. Poulson, and F. R. Hauer (2011), Tracing dissolved O2 and dissolved inorganic carbon stable isotope dynamics in the Nyack aquifer: Middle Fork Flathead River, Montana, USA, *Geochim. Cosmochim. Acta*, *75*(20), 5971–5986.

Sobczak, W. V., and S. Findlay (2002), Variation in bioavailability of dissolved organic carbon among stream hyporheic flow paths, *Ecology*, *83*, 3194–3209, doi:10.1890/0012-9658(2002)083[3194:VIBODO]2.0.CO;2.

Stanford, J. A., J. V. Ward, and B. K. Ellis (1994), Ecology of the alluvial aquifers of the Flathead River, Montana, in *Groundwater Ecology*, edited by J. Gilbert et al., pp. 367–390, Academic Press, San Diego, Calif.

Stanford, J. A., M. S. Lorang, and F. R. Hauer (2005), The shifting habitat mosaic of river ecosystems, *Verh. Int. Ver. Theor. Angew. Limnol.*, *29*, 123–136.

Starr, R. C., and R. W. Gillham (1993), Denitrification and organic carbon availability in two aquifers, *Groundwater*, *31*(6), 934–947, doi:10.1111/j.1745-6584.1993.tb00867.x.

Stedmon, C. A., and R. Bro (2008), Characterizing dissolved organic matter fluorescence with parallel factor analysis: A tutorial, *Limnol. Oceanogr. Methods*, *6*, 572–579.

Stedmon, C. A., and S. Markager (2005), Tracing the production and degradation of autochthonous fractions of dissolved organic matter by fluorescence analysis, *Limnol. Oceanogr.*, *50*, 1415–1426.

Stedmon, C. A., S. Markager, and R. Bro (2003), Tracing dissolved organic matter in aquatic environments using a new approach to fluorescence spectroscopy, *Mar. Chem.*, *82*, 239–254, doi:10.1016/S0304-4203(03)00072-0.

Strayer, D. L., S. E. May, P. Nielson, W. Wollheim, and S. Hausam (1997), Oxygen, organic matter and sediment granulometry as controls on hyporheic animal communities, *Arch. Hydrobiol.*, *140*, 131–144.

Trimmer, M., A. G. Hildrew, M. C. Jackson, J. L. Pretty, and J. Grey (2009), Evidence for the role of methane-derived carbon in a free-flowing, lowland river food web, *Limnol. Oceanogr.*, *54*(5), 1541–1547, doi:10.4319/lo.2009.54.5.1541.

Valett, H. M., F. R. Hauer, and J. A. Stanford (2014), Landscape influences on ecosystem function: Local and routing control of oxygen dynamics in a floodplain aquifer, *Ecosystems*, *17*(2), 195–211, doi:10.1007/s10021-013-9717-5.

Weishaar, J. L., G. R. Aiken, B. A. Bergamaschi, M. S. Fram, R. Fujii, and K. Mopper (2003), Evaluation of specific ultraviolet absorbance as an indicator of the chemical composition and reactivity of dissolved organic carbon, *Environ. Sci. Technol.*, *37*, 4702–4708, doi:10.1021/es030360x.

Whited, D. C., M. S. Lorang, M. J. Harner, F. R. Hauer, J. S. Kimball, and J. A. Stanford (2007), Climate, hydrologic disturbance, and succession: Drivers of floodplain pattern, *Ecology*, *88*, 940–953, doi:10.1890/05-1149.

Wickland, K. P., G. R. Aiken, K. Butler, M. M. Dornblaser, R. G. M. Spencer, and R. G. Striegl (2012), Biodegradability of dissolved organic carbon in the Yukon River and its tributaries: Seasonality and importance of inorganic nitrogen, *Global Biogeochemical Cycles*, *26*, GB0E03, doi:10.1029/2012GB004342.

Williams, D. D., and H. B. N. Hynes (1974), The occurrence of benthos deep in the substratum of a stream, *Freshwater Biol.*, *4*, 233–256, doi:10.1111/j.1365-2427.1974.tb00094.x.

Yates, T. T., B. C. Si, R. E. Farrell, and D. J. Pennock (2006), Probability distribution and spatial dependence of nitrous oxide emission: Temporal change in hummocky terrain, *Soil Sci. Soc. Am. J.*, *70*(3), 753–762, doi:10.2136/sssaj2005.0214.

Zarnetske, J. P., R. Haggerty, S. M. Wondzell, and M. A. Baker (2011), Dynamics of nitrate production and removal as a function of residence time in the hyporheic zone, *J. Geophys. Res.*, *116*, G01025, doi:10.1029/2010JG001356.